

Received 17 November 2018; revised 5 February 2019 and 11 March 2019; accepted 14 March 2019. Date of publication 28 March 2019; date of current version 17 April 2019.

Digital Object Identifier 10.1109/JTEHM.2019.2907945

# Deep Learning-Based Proarrhythmia Analysis Using Field Potentials Recorded From Human Pluripotent Stem Cells Derived Cardiomyocytes

ZEINAB GOLGOONI<sup>1</sup>, SARA MIRSADEGHI<sup>2</sup>, MAHDIEH SOLEYMANI BAGHSHAH<sup>1</sup>, PEDRAM ATAEE<sup>1</sup>, HOSSEIN BAHARVAND<sup>3,4</sup>, SARA PAHLAVAN<sup>3</sup>, AND HAMID R. RABIEE<sup>1</sup>

<sup>1</sup>Advanced ICT Innovation Center, Department of Computer Engineering, Sharif University of Technology, Tehran 145889694, Iran

<sup>2</sup>Cell Science Research Center, Department of Brain and Cognitive Science, Royan Institute for Stem Cell Biology and Technology, ACECR, Tehran 16635-148, Iran

<sup>3</sup>Cell Science Research Center, Department of Stem Cells and Developmental Biology, Royan Institute for Stem Cell Biology and Technology, ACECR, Tehran 16635-148, Iran

<sup>4</sup>Department of Developmental Biology, University of Science and Culture, Tehran 1461968151, Iran

This paper has supplementary downloadable material available at <http://ieeexplore.ieee.org>, provided by the author.

CORRESPONDING AUTHORS: M. SOLEYMANI BAGHSHAH ([soleymani@sharif.edu](mailto:soleymani@sharif.edu)) AND S. PAHLAVAN ([sarapahlavan@royaninstitute.org](mailto:sarapahlavan@royaninstitute.org))

This work was supported in part by the Royan Institute, in part by the Sharif University of Technology, through the Vice-Presidency of Research, in part by the National Elite Federation, and in part by the Sharif Advanced ICT Innovation Center.

**ABSTRACT** An early characterization of drug-induced cardiotoxicity may be possible by combining comprehensive *in vitro* proarrhythmia assay and deep learning techniques. We aimed to develop a method to automatically detect irregular beating rhythm of field potentials recorded from human pluripotent stem cells (hPSC) derived cardiomyocytes (hPSC-CM) by multi-electrode array (MEA) system. We included field potentials from 380 experiments, which were labeled as normal or arrhythmic by electrophysiology experts. Convolutional and recurrent neural networks (CNN and RNN) were employed for automatic classification of field potential recordings. A preparation phase was initially applied to split 60-s long recordings into a series of 5-s windows. Subsequently, the classification phase comprising of two main steps was designed and applied. The first step included the classification of 5-s windows by using a designated CNN. While, the results of 5-s window assessments were used as the input sequence to an RNN that aggregates these results in the second step. The output was then compared to electrophysiologist-level arrhythmia detection, resulting in 0.83 accuracy, 0.93 sensitivity, 0.70 specificity, and 0.80 precision. In summary, this paper introduces a novel method for automated analysis of “irregularity” in an *in vitro* model of cardiotoxicity experiments. Thus, our method may overcome the drawbacks of using predesigned features that restricts the classification performance to the comprehensiveness and the quality of the designed features. Furthermore, automated analysis may facilitate the quality control experiments through the procedure of drug development with respect to cardiotoxicity and avoid late drug attrition from market.

**INDEX TERMS** Arrhythmia detection, cardiomyocyte, CiPA, deep learning, hPSC.

## I. INTRODUCTION

Cardiotoxicity is one of the major reasons for drug attrition from market which may impose tremendous costs to pharmaceutical companies [1]. Drugs may impose side effects on structure or electrophysiology of cardiac myocytes. Comprehensive *in vitro* proarrhythmia assay (CiPA) using the hPSC-CM/MEA system have been proposed as a robust, efficient, and sensitive platform for electrophysiological

cardiotoxicity screenings [2]–[13]. While industry standard assays are based on using immortalized cell lines or animal models, CiPA takes the advantage of cardiomyocytes obtained from cardiogenic differentiation of hPSC, literally representing the most similar physiology to human heart [14]. Therefore, this high throughput physiologically relevant platform for cardiotoxicity [6] may provide an advanced complementary method with great potential for reducing the

costs of drug development and cardiotoxicity-related drug attrition. However, the implementation of CiPA initiative is highly dependent on necessary adjustments to this technique including generation of mature hPSC-CM as well as standard culture, differentiation and assay methods [8].

Field potentials recorded from hPSC-CM using MEA system is well correlated to action potentials recorded from single cardiomyocytes and electrocardiogram (ECG) recorded from the whole heart [15]. Furthermore, hPSC-CM/MEA platform could reliably demonstrate the cardiotoxicity of drugs which are known to be arrhythmogenic, according to previous reports [16]–[18]. Based on these findings, efforts have been made to generate a quantitative system in order to predict drugs with proarrhythmic risk [16], [19], [20].

By developing diverse experimental platforms and their quantitative readouts, scientists faced large datasets which required extensive human resource and time to perform the analyses and interpretation. Last few decades have been the golden age for the development of automated tasks to help experts and improve performance in the field of medical data analyses [21]–[25]. Especially, recent studies have proposed deep learning methods to overcome drawbacks of employing hand-engineered features to describe data characteristics. In fact, the deep learning methods do not explicitly require any type of feature design by human experts, and instead, the features are implicitly learned from data through an automatic learning procedure [26]. Recently, a few studies have investigated the task of analysis and classification of electrocardiogram (ECG) signals with deep learning methods [27], [28]. Kiranyaz *et al.* [27] and Pranav Rajpurkar *et al.* [28] introduced a deep learning model to classify ECG samples and could exceed the average cardiologists performance in both sensitivity and precision measures [28]. In another study, a personalized monitoring and warning system based on deep learning methods was designed for cardiac arrhythmia prediction [27].

Despite the development of new methods for automation of arrhythmia detection on surface ECG, the interpretation of data obtained from hPSC-CM/MEA system and the translation of findings for risk assessment is still in its infancy. Advanced machine learning methods can play an important role on creating computer-aided diagnosis (CAD) tools for hPSC-CM/MEA data analysis. In this study, we hypothesized that deep learning approach can be exploited to create a model for irregularity detection in the field potentials recorded from hPSC-CM. Our model was designed using two different networks namely CNN [29] and RNN [30] to classify signals of different durations, which resulted in proarrhythmia prediction with 0.83 accuracy.

## II. METHODS AND PROCEDURES

A novel approach for automated assessment of irregularity in the field potentials recorded from hPSC-CM is proposed. The recorded field potentials are classified into normal and arrhythmic using a specific deep learning method designed

for this purpose. The diagram of the proposed method is shown in Fig. 1. In this section, we first introduce the generation of hPSC-CM data. Then, the proposed deep learning model for classifying hPSC-CM data is presented.

### A. EXPERIMENTAL DATA

#### 1) GENERATION OF hPSC-CM

hPSC lines including hESC (RH5) [31] and hiPSC [32] were subjected to cardiogenic differentiation. In order to induce CM differentiation of hPSC in a suspension culture system, the 5-day-old size-controlled hPSC spheroids (average size:  $175 \pm 25 \mu\text{m}$ ) were cultured for 24 hours in differentiation medium (RPMI 1640 medium; Gibco) supplemented with 2% B-27 supplement without vitamin A (12587-010; Gibco), 2 mM L-glutamine (25030-024; Gibco), 0.1 mM  $\beta$ -mercaptoethanol (M7522; Sigma-Aldrich) and 1% nonessential amino acids (11140-035; Gibco) containing 12  $\mu\text{M}$  of CHIR99021 (a small molecule activating canonical Wnt/ $\beta$ -catenin pathway) (CHIR; 041-0004; Stemgent). The spheroids were subsequently washed with Dulbecco's phosphate-buffered saline (DPBS) and maintained in fresh differentiation medium without small molecule (SM) for one day. Thereafter, the medium was exchanged for new differentiation medium that contained 5  $\mu\text{M}$  IWP2 (3533; Tocris Bioscience) as a Wnt antagonist, 5  $\mu\text{M}$  SB431542 (S4317; Sigma-Aldrich) as an inhibitor of transforming growth factor- $\beta$  superfamily type I activin receptor-like kinase receptors, and 5  $\mu\text{M}$  purmorphamine (Pur; 04-0009; Stemgent) as a sonic hedgehog (SHH) agonist. The spheroids were cultured for 2 days in this medium, after which they were washed with DPBS and further cultured in a fresh differentiation medium without SMs. This medium was refreshed every 2–3 days.

Cardiomyocytes differentiated from two patient-specific hiPSC lines including CPVT1 and LQTS2 were used as test data. CPVT1 patient-specific iPSC line NP0014 (clone c6) [33, 34] and LQTS2 patient-specific iPSC line NP0011 (clone c8) [35] were provided by Dr. Juergen Hescheler (University of Cologne), have been deposited at the European Bank for induced pluripotent Stem Cells (EBiSC; <https://www.ebisc.org/>) and are registered at the online registry for human pluripotent stem cells hPSCreg (<https://hpscereg.eu/>) under the names UKKi007-A and UKKi009-A, respectively.

#### 2) APPLICATION OF CARDIOACTIVE DRUGS

We used a multi-electrode array (MEA) data acquisition system (Multichannel Systems) for extracellular field potential recordings. The MEA plates contained a matrix of 60 titanium nitride electrodes (30  $\mu\text{m}$ ) with an inter-electrode distance of 200  $\mu\text{m}$ . MEA plates were sterilized with 70% ethanol solution and hydrophilized with fetal bovine serum for 30 minutes, washed with sterile water, and then coated with an ECM gel from Engelbreth-Holm-Swarm mouse sarcoma (catalog no. E1270; Sigma-Aldrich). Beating spheroids were plated in differentiation medium on the middle of sterilized

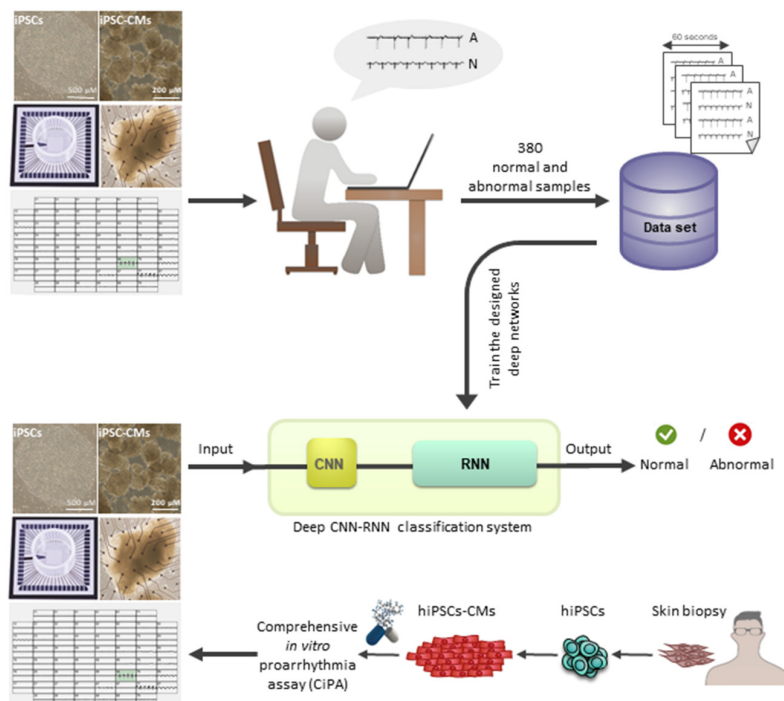


**FIGURE 1. Deep learning based proarrhythmia analysis for cardiac safety pharmacology.** We constructed a dataset from FP recordings of hPSC-CM using MEA system. The dataset contained 380 samples of 60-second long recordings. Each record was labeled as normal or abnormal by electrophysiology experts. Using the provided dataset, we trained the proposed deep architecture composed of CNN and RNN networks that was designed for binary classification of data. This trained deep CNN-RNN system can be further used for classification of new FP recordings into normal and abnormal categories specially in comprehensive *in vitro* proarrhythmia assay.

matrigel-coated MEA plates for at least 48 hours to allow proper attachment. On the day of the experiment, the MEA plates were connected to a head stage amplifier. The recordings were performed for 60 seconds at baseline. Samples with beating frequencies of  $70 \pm 15$  beats per minute (bpm) were selected for the rest of the experiments and other beating spheroids with higher or lower rates were excluded due to heterogeneity of samples and diversity of their normal beating rates. This initial filtering was applied in order to avoid the possible interference of diversified beating frequencies of hPSC-CM in automated arrhythmia detection. In order to induce arrhythmic-like events and mimic drug-induced arrhythmia, cardioactive drugs were applied on hPSC-CM and field potential recordings were performed 5 minutes after drug application. Verapamil hydrochloride (Sigma-Aldrich) at concentration range of 100-200 nM, Nifedipine (Sigma-Aldrich) at concentration range of 50-100 nM, Isoproterenol hydrochloride (Sigma-Aldrich) at concentration of  $5 \mu\text{M}$ , Propranolol hydrochloride (Sigma-Aldrich) at concentration of  $10 \mu\text{M}$  and Sotalol hydrochloride (Sigma-Aldrich) at concentration range of 100-500  $\mu\text{M}$  were used. All recordings were performed at  $37^\circ\text{C}$ . The extracellular field potentials were sampled at 2 KHz in Cardio2D software (V 2.6.2; Multichannel Systems) and saved for further analysis.

### 3) DATA PREPARATION

To provide input signals to train and test the model, we used normal and arrhythmic field potentials recorded from hPSC-CM. Field potential recordings from 380 experiments were carefully studied and labeled by two electrophysiology experts. These data were categorized into normal and arrhythmic based on several parameters such as beating rates, field potential durations, and polymorphic waveforms, thus making this labeling process a time-consuming analysis. It has to be noted that the above mentioned parameters are to a large extent dependent on the cell line of interest [8] including hESC-CM or normal as well as patient-specific hiPSC-CM. Furthermore, there are a high line-to-line variability in beating frequencies of differentiated cardiomyocytes. Thus, we tried to establish as much homogeneity as possible in train and test data by excluding heterogeneous samples as stated in Section 2. In order to prepare signals for the classification task, they were initially subjected to preprocessing steps, i.e., smoothing and windowing.

First, each raw signal was normalized using Min-Max technique and smoothing using a moving average filter in BioSppy library [36] to reduce noise. Then, the preprocessed 60-second long signals were windowed into a series of 5-second windows, each started at a particular R-peak and continued to the fixed length of 5 seconds (Fig. 2).

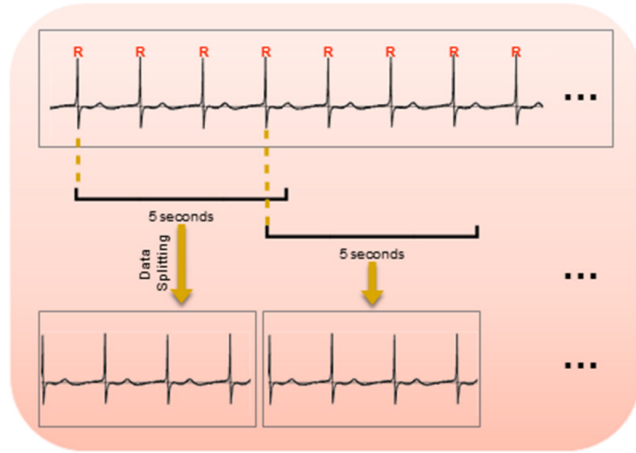


**FIGURE 2.** Splitting a 60-second long recording into a sequence of 5-second long windows. To split a record, R peaks are detected all over the recording. Each 5-second long window starts from a particular R point and continues to the fixed length of five seconds.

### B. CLASSIFICATION MODEL

After the preparation phase, the preprocessed data were classified into normal or arrhythmic using a 2-step deep learning method. The architecture of the proposed model is shown in Fig. 3.

In the first step, we employ a specific 1-D CNN architecture that works on the preprocessed data as its input without employing any predesigned feature such as field potential duration, beating duration (R-R interval), and beating rate. The input layer size was 5000 that was determined based upon the number of 5-second long windows sampled at 1 KHz. The CNN contained 3 layers of convolution each of which included 16 kernels of size 80. Indeed, each filter (consisting of 80 trainable parameters) convolves with the sequence of features obtained in the previous layer (or with the input sequence for the first convolutional layer). After the convolutional layers which were designated to extract features from the input signal, one fully-connected layer with the sigmoid activation function was used to generate the output specifying the probability of arrhythmicity for the corresponding window (details about the designated model is presented below).

The second step was allocated to classification of the whole field potential recording, based on the sequence of evaluation results obtained on the 5-second long windows. For this purpose, the well-known Long Short Term Memory (LSTM) [37], as an RNN architecture, was employed. The designed network contained one recurrent layer with three neurons and one fully-connected layer. In fact, the RNN network can process the sequence of evaluations obtained on 5-second long windows by CNN in the previous step and aggregate them to reach the final decision.

To train the proposed model composed of the CNN and RNN, we used our dataset including both normal and arrhythmic field potential recordings of hPSC-CM that was previously labeled by electrophysiologists.

### DETAILS OF THE NETWORK ARCHITECTURE

The details of the proposed deep architecture are shown in Tables 1 and 2. The first part of the model is composed of a 1-D CNN architecture that is applied on the input layer with size of 5000. This network consists of three convolutional layers, each had 16 filters with the kernel size of 80 and finally includes one fully-connected layer. The activation functions that are performed after convolutional layers, are chosen to be Relu and the activation function used after the fully connected layer is selected to be the sigmoid function. Moreover, after each convolutional layer and before the activation function, batch normalization [38] is adopted to provide more stable training. We also use dropout [39] at each convolution layer to improve the generalization capability of the proposed algorithm.

**TABLE 1.** The designed CNN architecture.

<i>Input size = 5000</i>
<b>1D Convolution:</b> no. of filters = 16, kernel size = 80, stride = 2
<b>Batch normalization</b>
<b>Activation function:</b> Relu
<b>Max Pooling 1D</b>
<b>Dropout:</b> rate = 0.5
<b>1D Convolution:</b> no. of filters = 16, kernel size = 80, stride = 2
<b>Batch normalization</b>
<b>Activation function:</b> Relu
<b>Dropout:</b> rate = 0.5
<b>1D Convolution:</b> no. of filters = 16, kernel size = 80, stride = 2
<b>Batch normalization</b>
<b>Activation function:</b> Relu
<b>Max Pooling 1D</b>
<b>Dropout:</b> rate = 0.5
<b>Dense:</b> no. of neurons= 1
<b>Activation function:</b> sigmoid

**TABLE 2.** The designed RNN architecture.

<i>input shape = a sequence</i>
<b>LSTM layer</b> (no. of nodes = 3, kernel initializer = 1)
<b>Batch normalization</b>
<b>Activation function:</b> Relu
<b>Dropout:</b> rate = 0.5
<b>Dense:</b> no. of neurons= 1
<b>Activation function:</b> sigmoid

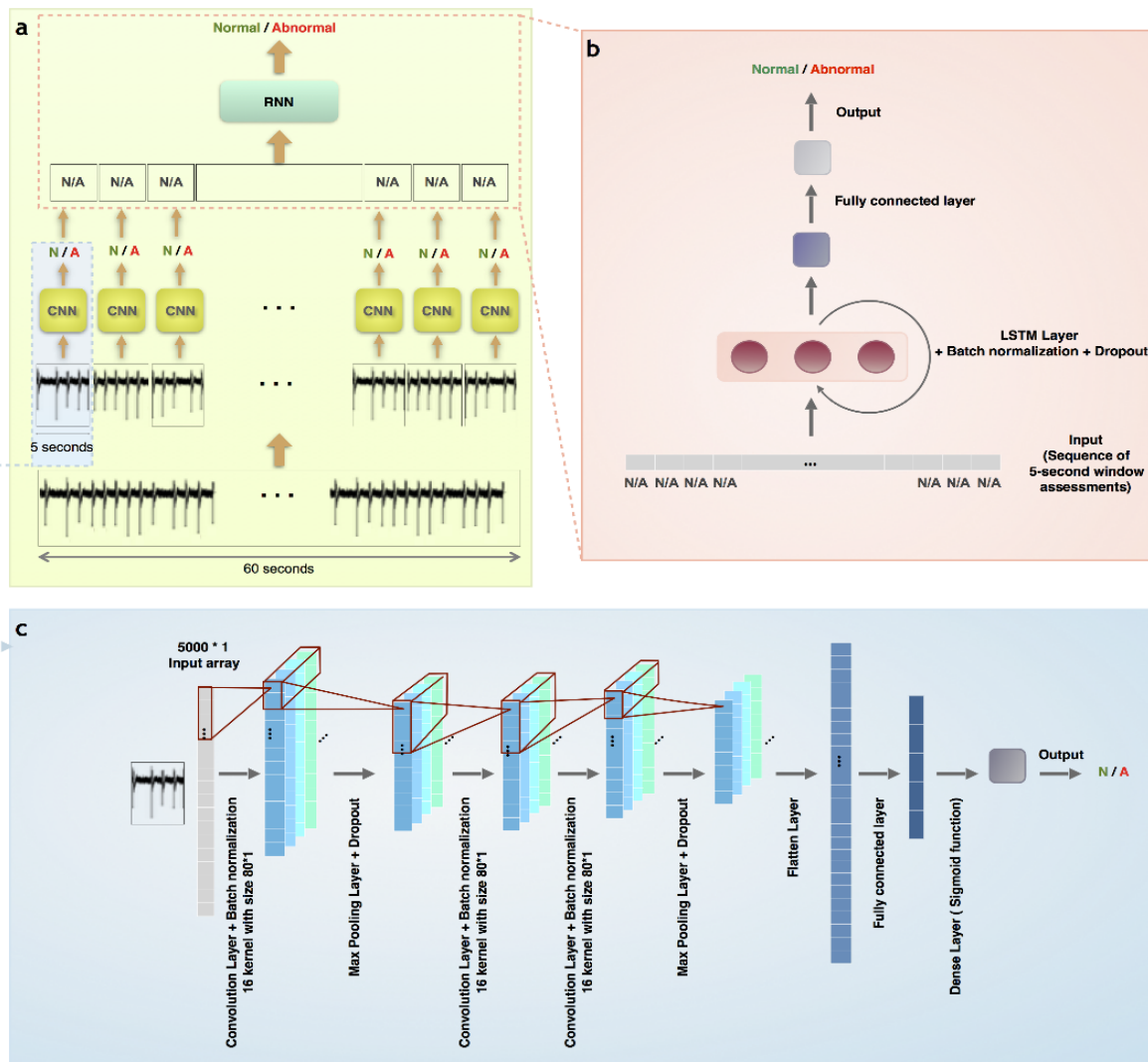


**FIGURE 3.** Representation of the two-step deep learning-based classification model. a) The general architecture of the proposed method: To classify a field potential recording of hPSC-CM, a primary denoising followed by splitting of the 60-second long recording into the set of 5-second signals is applied. Each 5-second-long window is fed into the trained CNN (the details of the CNN architecture was shown in (b)) which produces output results for that window. Then, the sequence of CNN outputs is used as the input for the trained RNN (its components were presented in (c)). The RNN output determined our final result given the decisions of CNN on the 5-second signals, classifying the 60-second long field potential recording as normal or arrhythmic. Abbreviations: N; Normal and A; Arrhythmic. b) The CNN architecture that takes 5-second long window as input and provides assessment of that window (probability of being normal or arrhythmic for 5-second long window). c) The RNN architecture that takes the sequence of 5-second long windows assessments as the input and provide the final result (probability of being normal or abnormal for 60-second long recording).

The second part of the proposed model is an RNN that prepares the final output. It consists of one recurrent layer (LSTM architecture) with three neurons and one fully-connected layer with the sigmoid activation function. In addition, batch normalization and dropout are also applied in the recurrent layer. The activation function in the recurrent layer is set to Relu.

We use the Adam optimizer for training both CNN and RNN. The number of epochs is set to be 100. Moreover, 5-fold cross-validation is utilized to tune hyper-parameters of the proposed model (e.g. the rate of dropout, the kernel size of convolutional layers, and etc.)

### III. PERFORMANCE MEASURES

To evaluate the proposed method, the following performance measures as the most commonly used measures are utilized:

$$\text{Accuracy} = \frac{\# \text{Samples correctly classified}}{\# \text{All inputs samples}} \quad (1)$$

$$\text{Sensitivity} = \frac{\# \text{Abnormal samples correctly classified}}{\# \text{All abnormal samples}} \quad (2)$$

$$\text{Specificity} = \frac{\# \text{Normal samples correctly classified}}{\# \text{All normal samples}} \quad (3)$$

$$\text{Precision} = \frac{\# \text{Abnormal samples correctly classified}}{\# \text{All samples classified as abnormal}} \quad (4)$$

$$F \text{ score} = \frac{2 \times \text{recall} \times \text{precision}}{\text{recall} + \text{precision}} \quad (5)$$

where Accuracy shows the proportion of correctly classified samples to the whole number of samples. Moreover, Sensitivity indicates the proportion of samples correctly classified as abnormal to the whole number of abnormal samples. On the other hand, Specificity shows the proportion of samples correctly classified as normal to the whole number of normal samples. Precision denotes the proportion of correctly classified abnormal samples to the whole number of samples that are classified as abnormal. Finally, F score shows the harmonic mean of the Precision and Recall (or Sensitivity).

#### IV. RESULTS

In this study, we developed a new classification model to automatically identify normal and arrhythmic field potential waveforms of human cardiomyocytes differentiated from hPSC and subjected to cardioactive drugs (Fig. 1).

The healthy hPSC-CM were generated using a small molecule-based differentiation protocol [40]–[42]. The spheroids of 30-day old hPSC-CM were plated on the electrodes of a multielectrode array system and their field potential recordings were performed (Supplementary movie 1) [40], [42]. The field potentials recorded from multi-cellular spheroids of hPSC-CM resembled the surface ECG recorded from the whole heart (Supplementary Fig. S1) and provided valuable information on the excitability and functionality of differentiated cardiomyocytes. The field potential waveform included data on the duration of a beating cycle (R-R interval), the field potential duration (FPD) which correlates to repolarization phase of the action potential and QT interval of ECG, and the field potential rhythmicity (Supplementary Fig. S2). We also applied some known cardioactive drugs with acute effects on healthy hPSC-CM in order to experimentally mimic arrhythmogenesis and to only provide raw data for the development of classifier. Therefore, we are not going to discuss the drug effects in this paper.

We collected a dataset of 380 field potential recordings obtained from healthy hPSC-CM as well as their cardioactive drugs experiments to be used in this study. These experiments helped the formation of a large dataset with valuable information but time-consuming and difficult to be manually analyzed. Furthermore, the *in vitro* cardiotoxicity assay using hPSC-CM and MEA system is a novel approach which lacks sufficient and appropriate analysis software.

Although efforts have been made to develop analysis tools [19], [20], to the best of our knowledge, there has not been any published results on the automatic classification of field potential recordings from hPSC-CM into normal or arrhythmic.

These 380 recordings were labeled as normal and arrhythmic waveforms by electrophysiology experts based on pre-designed metrics such as beating rates and/or FPD (Fig. 4). The arrhythmic waveforms included long FPD, bradycardia, tachycardia, and polymorphic (Fig. 5). We used 20% of this dataset as the test set and 80% for training and

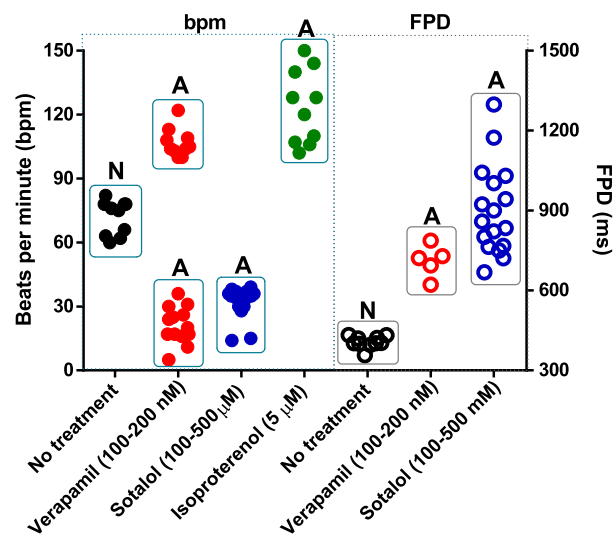


**FIGURE 4.** Labeling of field potential recordings from hPSC-CM at baseline and when subjected to treatment with cardioactive agents. N; normal ( $\text{bpm} = 70 \pm 15$  and  $\text{FPD} = 400 \pm 50$  ms), A; arrhythmic ( $45 \leq \text{bpm} \leq 100$  and  $\text{FPD} \geq 600$  ms).

validation of the classification method. A few recordings from patient-specific hiPSC-CM including CPVT1 and LQTS2 were also used as test data to further evaluate the classification model. The 60s long recordings were windowed to 5s long field potential recordings (Fig. 2). By this method, we created 7000 5s-long input signals.

Following the training of CNN by these 5s long recordings, the RNN was trained to aggregate output results of CNN for each 60s long waveform (Fig. 3). The final trained networks were saved for further classification of test signals as well as any other input signal. The results of classification by deep learning-based classifier on the test data showed the performance metrics of 0.83 accuracy (Eq. 1), 0.93 sensitivity (Eq. 2), 0.70 specificity (Eq. 3), and 0.80 precision (Eq. 4) on the test dataset. In addition, the F-score as a harmonic mean of sensitivity and precision (Eq. 5), was also evaluated to be 0.86.

Therefore, the proposed classification method has resulted in a considerable performance without using the expert knowledge for designing the features and the classification system.

#### V. DISCUSSION

The CiPA proposes a cardiotoxicity screening schema that results in a more robust, efficient, and sensitive system avoiding a late drug attrition from the market [14]. The hPSC-CM constituted a valuable tool for validating *in silico* reconstruction of proarrhythmic risk throughout the process of drug development. Therefore, the functional assays representing the excitability or contractile function of these cells as well as advanced techniques for data analysis would be an important complement to CiPA.

The introduction of combined hPSC-CM technology and MEA system for drug discovery and cardiotoxicity assays

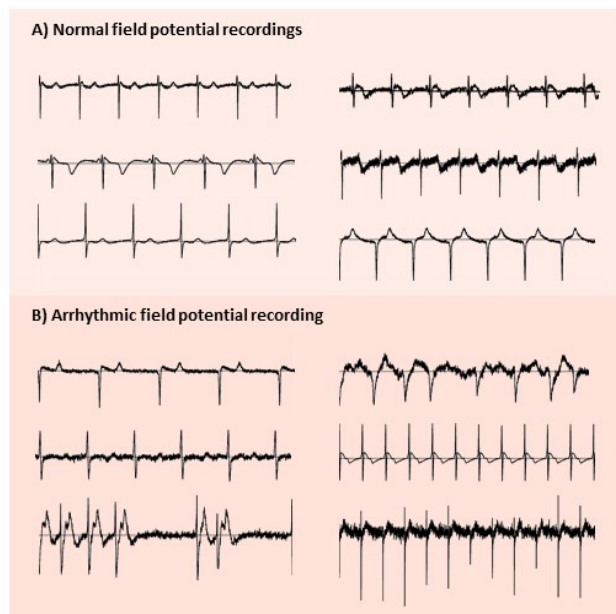


**FIGURE 5.** Representative extracellular field potential recordings of hPSC-CM. A) 5-second long recordings labeled as normal. B) 5-second long traces labeled as arrhythmic due to the observed phenotypes such as long FPD, bradycardia, and polymorphic waveforms.

has encouraged many scientists to test this platform and analyze its output signals [7], [8], [42]–[47]. Especially, this system is developed to be employed in a high-throughput drug screening platform with major needs of automated and sensitive analysis tools. Despite complexity, MEA output signals received more accurate interpretation by application of simulation methods to more precisely profile field potentials with respect to its underlying action potentials [48], thus providing the basis for more reliable and advanced analysis of drug toxicity screenings. However, the automation of cardiotoxicity characterization as proarrhythmic effects is still missing.

Over the last few years, the majority of analysis tools were developed for calculating the field potential parameters. Pradhapen and coworkers developed a semi-automatic software for analysis of field potentials recorded from iPSC-CM [20]. Their offline software called cardioMD had correlation analysis and ensemble averaging features which were used to reliably analyze the field potential durations and providing an output waveform for the expert to manually determine various morphology changing signals.

In another approach, the waveforms obtained from impedance measurements of iPSC-CM were subjected to a mathematical model (hCAR) for arrhythmic risk assessment [19]. The hCAR model could successfully bridge the gap between hERG screening system and *in vivo* QT prolongation as well as arrhythmia assessment in preclinical and clinical studies.

Furthermore, cytotoxic factors could be identified and rank-ordered using hCAR model. However, it employed

some defined parameters and mathematical equations to predict proarrhythmia risk, thus limiting the power of analysis to the proposed features. In contrast, we developed a deep learning-based analysis tool that is able to use a broad range of field potential features which resulted in arrhythmia assessment by monitoring morphological changes rather than application of any preselected features.

Deep learning based models have shown significant results and are known as state-of-the-art methods for many tasks of medical image analysis [25] and biological data analysis [49].

We proposed a two-step deep learning model composed of CNN and RNN to classify field potential recordings. First step consists of a CNN that integrates the feature extraction and classification phases by learning both the representation and the classifier jointly. It finds the (normal/abnormal) label for the fixed duration windows of input data. Second step consists of an RNN that enables the analysis of recordings with various lengths (>5 seconds). By using RNN, we are able to process and aggregate the sequence of results obtained for the small windows (as the output of CNN in the first step of the model) with no limit on the length of field potential recordings. Therefore, our model can process raw multielectrode array data of various lengths, and do not require to use predesigned features. Thus, it can overcome the drawbacks of using predesigned features that restricts the classification performance to the comprehensiveness and the quality of the designed features. Using the proposed method, we achieved 83% accuracy to identify normal and arrhythmic waveforms.

Additionally, the performance of the proposed model can be improved by increasing the size of dataset since the deep learning methods can show their real capability when they are trained on large datasets. Moreover, the binary classification can be easily extended to multi-class classification if larger datasets are used.

## VI. CONCLUSION

The proposed two-step CNN-RNN model provides an efficient, sensitive, and accurate platform for analysis and interpretation of hPSC-CM/MEA datasets which may facilitate the preclinical cardiac safety pharmacology through CiPA. In fact, in the proposed method, we do not need any expert knowledge for predesigning features and the proposed network that is trained end-to-end can work on raw signals. The proposed deep network was designed to classify the signals of different lengths using a combination of CNN and RNN networks.

## APPENDIX

The link to the program execution is presented below.

“<https://github.com/zGolgooni/Deep-CNN-RNN-for-iPSC-CMs>”.

## ACKNOWLEDGMENT

The authors would like to thank Dr. Maryam Barekat for her time and assistance in cardiologist-based arrhythmia detec-

tion. They would also like to thank Dr. Anna Meyfour for her kind help in preparing figures.

## REFERENCES

- [1] N. Ferri, P. Siegl, A. Corsini, J. Herrmann, A. Lerman, and R. Benghozi, "Drug attrition during pre-clinical and clinical development: understanding and managing drug-induced cardiotoxicity," *Pharmacol. Therapeutics*, vol. 138, no. 3, pp. 470–484, 2013. doi: [10.1016/j.pharmthera.2013.03.005](https://doi.org/10.1016/j.pharmthera.2013.03.005).
- [2] A. Mehta, Y. Chung, G. L. Sequiera, P. Wong, R. Liew, and W. Shim, "Pharmacoelectrophysiology of viral-free induced pluripotent stem cell-derived human cardiomyocytes," *Toxicol. Sci.*, vol. 131, no. 2, pp. 458–469, 2013. doi: [10.1093/toxsci/kfs309](https://doi.org/10.1093/toxsci/kfs309).
- [3] M. Clements and N. Thomas, "High-throughput multi-parameter profiling of electrophysiological drug effects in human embryonic stem cell derived cardiomyocytes using multi-electrode arrays," *Toxicol. Sci.*, vol. 140, no. 2, pp. 445–461, 2014. doi: [10.1093/toxsci/kfu084](https://doi.org/10.1093/toxsci/kfu084).
- [4] M. Clements, V. Millar, A. S. Williams, and S. Kalinka, "Bridging functional and structural cardiotoxicity assays using human embryonic stem cell-derived cardiomyocytes for a more comprehensive risk assessment," *Toxicol. Sci.*, vol. 148, no. 1, 2015, pp. 241–260. doi: [10.1093/toxsci/kfv180](https://doi.org/10.1093/toxsci/kfv180).
- [5] K. Harris, "A human induced pluripotent stem cell-derived cardiomyocyte (hiPSC-CM) multielectrode array assay for preclinical cardiac electrophysiology safety screening," *Current Protocols Pharmacol.*, vol. 71, no. 1, pp. 11–18, 2015. doi: [10.1002/0471141755.ph1118s71](https://doi.org/10.1002/0471141755.ph1118s71).
- [6] A. Maillet et al., "Modeling doxorubicin-induced cardiotoxicity in human pluripotent stem cell derived-cardiomyocytes," *Sci. Rep.*, vol. 6, May 2016, Art. no. 25333. doi: [10.1038/srep25333](https://doi.org/10.1038/srep25333).
- [7] L. Sala, D. W.-V. Oostwaard, L. G. J. Tertoolen, C. L. Mummery, and M. Bellin, "Electrophysiological analysis of human pluripotent stem cell-derived cardiomyocytes (hPSC-CMs) using multi-electrode arrays (MEAs)," *J. Vis. Exp.*, no. 123, 2017, Art. no. 55587. doi: [10.3791/55587](https://doi.org/10.3791/55587).
- [8] L. Sala, M. Bellin, and C. L. Mummery, "Integrating cardiomyocytes from human pluripotent stem cells in safety pharmacology: Has the time come?" *Brit. J. Pharmacol.*, vol. 174, no. 21, pp. 3749–3765, 2017. doi: [10.1111/bph.13577](https://doi.org/10.1111/bph.13577).
- [9] Y. Nozaki et al., "CSAHi study-2: Validation of multi-electrode array systems (MEA60/2100) for prediction of drug-induced proarrhythmia using human iPSC cell-derived cardiomyocytes: Assessment of reference compounds and comparison with non-clinical studies and clinical information," *Regulatory Toxicol. Pharmacol.*, vol. 88, pp. 238–251, Aug. 2017. doi: [10.1016/j.yrtph.2017.06.006](https://doi.org/10.1016/j.yrtph.2017.06.006).
- [10] G. Gintant, B. Fermini, N. Stockbridge, and D. Strauss, "The evolving roles of human iPSC-derived cardiomyocytes in drug safety and discovery," *Cell Stem Cell*, vol. 21, no. 1, pp. 14–17, 2017. doi: [10.1016/j.stem.2017.06.005](https://doi.org/10.1016/j.stem.2017.06.005).
- [11] J. Vicente et al., "Mechanistic model-informed proarrhythmic risk assessment of drugs: Review of the 'CiPA' initiative and design of a prospective clinical validation study," *Clin. Pharmacol. Therapeutics*, vol. 103, no. 1, pp. 54–66, 2018. doi: [10.1002/cpt.896](https://doi.org/10.1002/cpt.896).
- [12] J. Vicente, M. Hosseini, L. Johannesen, and D. G. Strauss, "Electrocardiographic biomarkers to confirm drug's electrophysiological effects used for proarrhythmic risk prediction under CiPA," *J. Electrocardiol.*, vol. 50, no. 6, pp. 808–813, 2017. doi: [10.1016/j.jelectrocard.2017.08.003](https://doi.org/10.1016/j.jelectrocard.2017.08.003).
- [13] X. Ligneau et al., "Nonclinical cardiovascular safety of pitolisant: Comparing international conference on harmonization S7B and comprehensive *in vitro* pro-arrhythmia assay initiative studies," *Brit. J. Pharmacol.*, vol. 174, no. 23, pp. 4449–4463, 2017. doi: [10.1111/bph.14047](https://doi.org/10.1111/bph.14047).
- [14] G. Gintant, P. T. Sager, and N. Stockbridge, "Evolution of strategies to improve preclinical cardiac safety testing," *Nature Rev. Drug Discovery*, vol. 15, no. 7, pp. 457–471, 2016. doi: [10.1038/nrd.2015.34](https://doi.org/10.1038/nrd.2015.34).
- [15] K. Banach, M. D. Halbach, P. Hu, J. Hescheler, and U. Egert, "Development of electrical activity in cardiac myocyte aggregates derived from mouse embryonic stem cells," *Amer. J. Physiol.-Heart Circulatory Physiol.*, vol. 284, no. 6, pp. 2114–2123, 2003. doi: [10.1152/ajp-heart.01106.2001](https://doi.org/10.1152/ajp-heart.01106.2001).
- [16] L. Guo et al., "Estimating the risk of drug-induced proarrhythmia using human induced pluripotent stem cell-derived cardiomyocytes," *Toxicol. Sci.*, vol. 123, no. 1, pp. 281–289, 2011. doi: [10.1093/toxsci/kfr158](https://doi.org/10.1093/toxsci/kfr158).
- [17] O. Caspi et al., "In vitro electrophysiological drug testing using human embryonic stem cell derived cardiomyocytes," *Stem Cells Develop.*, vol. 18, no. 1, pp. 161–172, 2009. doi: [10.1089/scd.2007.0280](https://doi.org/10.1089/scd.2007.0280).
- [18] S. R. Braam and C. L. Mummery, "Human stem cell models for predictive cardiac safety pharmacology," *Stem Cell Res.*, vol. 4, no. 3, pp. 155–156, 2010. doi: [10.1016/j.scr.2010.04.008](https://doi.org/10.1016/j.scr.2010.04.008).
- [19] L. Guo, L. Coyle, R. M. C. Abrams, R. Kemper, E. T. Chiao, and K. L. Kolaja, "Refining the human iPSC-cardiomyocyte arrhythmic risk assessment model," *Toxicol. Sci.*, vol. 136, no. 2, pp. 581–594, 2013. doi: [10.1093/toxsci/kft205](https://doi.org/10.1093/toxsci/kft205).
- [20] P. Pradhapan, J. Kuusela, J. Viik, K. Aalto-Setälä, and J. Hyttinen, "Cardiomyocyte MEA data analysis (CardioMDA)—a novel field potential data analysis software for pluripotent stem cell derived cardiomyocytes," *PLoS ONE*, vol. 8, no. 9, 2013, Art. no. e73637. doi: [10.1371/journal.pone.0073637](https://doi.org/10.1371/journal.pone.0073637).
- [21] D. F. Hayes, H. S. Markus, R. D. Leslie, and E. J. Topol, "Personalized medicine: Risk prediction, targeted therapies and mobile health technology," *BMC Med.*, vol. 12, no. 1, p. 37, 2014. doi: [10.1186/1741-7015-12-37](https://doi.org/10.1186/1741-7015-12-37).
- [22] H. M. Krumholz, "Big data and new knowledge in medicine: The thinking, training, and tools needed for a learning health system," *Health Affairs*, vol. 33, no. 7, pp. 1163–1170, 2014. doi: [10.1377/hlthaff.2014.0053](https://doi.org/10.1377/hlthaff.2014.0053).
- [23] S. B. Scruggs et al., "Harnessing the heart of big data," *Circulat. Res.*, vol. 116, no. 7, pp. 1115–1119, 2015. doi: [10.1161/CIRCRESAHA.115.306013](https://doi.org/10.1161/CIRCRESAHA.115.306013).
- [24] R. C. Deo, "Machine learning in medicine," *Circulation*, vol. 132, no. 20, pp. 1920–1930, 2015. doi: [10.1161/CIRCULATIONAHA.115.001593](https://doi.org/10.1161/CIRCULATIONAHA.115.001593).
- [25] G. Litjens et al. (2017). "A survey on deep learning in medical image analysis." [Online]. Available: <https://arxiv.org/abs/1702.05747>
- [26] Y. LeCun, Y. Bengio, G. Hinton, "Deep learning," *Nature*, vol. 521, no. 7553, pp. 436–444, 2015. doi: [10.1038/nature14539](https://doi.org/10.1038/nature14539).
- [27] S. Kiranyaz, T. Ince, and M. Gabbouj, "Personalized monitoring and advance warning system for cardiac arrhythmias," *Sci. Rep.*, vol. 7, no. 1, 2017, Art. no. 9270. doi: [10.1038/s41598-017-09544-z](https://doi.org/10.1038/s41598-017-09544-z).
- [28] P. Rajpurkar, A. Y. Hannun, M. Haghighpanahi, C. Bourn, and A. Y. Ng. (2017). "Cardiologist-level arrhythmia detection with convolutional neural networks." [Online]. Available: <https://arxiv.org/abs/1707.01836>
- [29] B. Y. Y. LeCun, "The handbook of brain theory and neural networks," *The Handbook of Brain Theory and Neural Networks*. Cambridge, MA, USA: MIT Press, 1998, pp. 255–258.
- [30] A. Graves, *Supervised Sequence Labelling With Recurrent Neural Networks*. Springer, 2012.
- [31] H. Baharvand et al., "Generation of new human embryonic stem cell lines with diploid and triploid karyotypes," *Develop., Growth Differentiation*, vol. 48, no. 2, pp. 117–128, 2006. doi: [10.1111/j.1440-169X.2006.00851.x](https://doi.org/10.1111/j.1440-169X.2006.00851.x).
- [32] A. Seifinejad et al., "Generation of human induced pluripotent stem cells from a Bombay individual: Moving towards 'universal-donor' red blood cells," *Biochem. Biophys. Res. Commun.*, vol. 391, no. 1, pp. 329–334, 2010. doi: [10.1016/j.bbrc.2009.11.058](https://doi.org/10.1016/j.bbrc.2009.11.058).
- [33] A. Fatima et al., "In vitro modeling of ryanodine receptor 2 dysfunction using human induced pluripotent stem cells," *Cell Physiol. Biochem.*, vol. 28, no. 4, pp. 579–592, 2011. doi: [10.1159/000335753](https://doi.org/10.1159/000335753).
- [34] X. H. Zhang et al., "Ca<sup>2+</sup> signaling in human induced pluripotent stem cell-derived cardiomyocytes (iPS-CM) from normal and catecholaminergic polymorphic ventricular tachycardia (CPVT)-afflicted subjects," *Cell Calcium*, vol. 54, no. 2, pp. 57–70, 2013. doi: [10.1016/j.ceca.2013.04.004](https://doi.org/10.1016/j.ceca.2013.04.004).
- [35] A. Fatima et al., "Generation of human induced pluripotent stem cell line from a patient with a long QT syndrome type 2," *Stem Cell Res.*, vol. 16, no. 2, pp. 304–307, 2016. doi: [10.1016/j.scr.2015.12.039](https://doi.org/10.1016/j.scr.2015.12.039).
- [36] C. Carreiras et al. (2015). BioSPPy—Biosignal Processing in Python. Python. [Online]. Available: <https://github.com/PIA-Group/BioSPPy>
- [37] S. Hochreiter and J. Schmidhuber, "Long short-term memory," *Neural Comput.*, vol. 9, no. 8, pp. 1735–1780, 1997.
- [38] S. Ioffe and C. Szegedy, "Batch normalization: Accelerating deep network training by reducing internal covariate shift," in *Proc. Int. Conf. Mach. Learn.*, 2015, pp. 448–456.
- [39] N. Srivastava, G. Hinton, A. Krizhevsky, I. Sutskever, and R. Salakhutdinov, "Dropout: A simple way to prevent neural networks from overfitting," *J. Mach. Learn. Res.*, vol. 15, no. 1, pp. 1929–1958, 2014.

- [40] H. Fonoudi *et al.*, “A universal and robust integrated platform for the scalable production of human cardiomyocytes from pluripotent stem cells,” *Stem Cells Transl. Med.*, vol. 4, no. 12, pp. 1482–1494, 2015. doi: [10.5966/sctm.2014-0275](https://doi.org/10.5966/sctm.2014-0275).
- [41] H. Fonoudi *et al.*, “Large-scale production of cardiomyocytes from human pluripotent stem cells using a highly reproducible small molecule-based differentiation protocol,” *J. Vis. Exp.*, no. 113, 2016, Art. no. 54276. [Online]. Available: <https://www.ncbi.nlm.nih.gov/pubmed/27500408>. doi: [10.3791/54276](https://doi.org/10.3791/54276).
- [42] S. Pahlavan *et al.*, “Effects of hawthorn (*Crataegus pentagyna*) leaf extract on electrophysiologic properties of cardiomyocytes derived from human cardiac arrhythmia-specific induced pluripotent stem cells,” *FASEB J.*, vol. 32, no. 3, pp. 1440–1451, 2018. doi: [10.1096/fj.201700494RR](https://doi.org/10.1096/fj.201700494RR).
- [43] D. Malan *et al.*, “Human iPSC cell model of type 3 long QT syndrome recapitulates drug-based phenotype correction,” *Basic Res. Cardiol.*, vol. 111, no. 2, p. 14, 2016. doi: [10.1007/s00395-016-0530-0](https://doi.org/10.1007/s00395-016-0530-0).
- [44] E. G. Navarrete *et al.*, “Screening drug-induced arrhythmia using human induced pluripotent stem cell-derived cardiomyocytes and low-impedance microelectrode arrays,” *Circulation*, vol. 128, no. 11, pp. S3–S13, 2013. doi: [10.1161/CIRCULATIONAHA.112.000570](https://doi.org/10.1161/CIRCULATIONAHA.112.000570).
- [45] F. Stillitano *et al.*, “Modeling susceptibility to drug-induced long QT with a panel of subject-specific induced pluripotent stem cells,” *Elife*, vol. 6, Jan. 2017, Art. no. e19406. doi: [10.7554/eLife.19406](https://doi.org/10.7554/eLife.19406).
- [46] J. Kuusela, J. Kim, E. Räsänen, and K. Aalto-Setälä, “The effects of pharmacological compounds on beat rate variations in human long QT-syndrome cardiomyocytes,” *Stem Cell Rev. Rep.*, vol. 12, no. 6, pp. 698–707, 2016. doi: [10.1007/s12015-016-9686-0](https://doi.org/10.1007/s12015-016-9686-0).
- [47] J. Kuusela *et al.*, “Effects of cardioactive drugs on human induced pluripotent stem cell derived long QT syndrome cardiomyocytes,” *SpringerPlus*, vol. 5, p. 234, Dec. 2016. doi: [10.1186/s40064-016-1889-y](https://doi.org/10.1186/s40064-016-1889-y).
- [48] L. G. J. Tertoolen, S. R. Braam, B. J. van Meer, R. Passier, and C. L. Mummery, “Interpretation of field potentials measured on a multi electrode array in pharmacological toxicity screening on primary and human pluripotent stem cell-derived cardiomyocytes,” *Biochem. Biophys. Res. Commun.*, vol. 497, no. 4, pp. 1135–1141, 2018. doi: [10.1016/j.bbrc.2017.01.151](https://doi.org/10.1016/j.bbrc.2017.01.151).
- [49] S. Min, B. Lee, and S. Yoon, “Deep learning in bioinformatics,” *Briefings Bioinf.*, vol. 18, no. 5, pp. 851–869, 2017.